Title
SINTERING OF SPHERICAL GLASS PONDER UNDER A UN1AXIAL STRESS

Authors
Rahaman, M.N
BeJonqhe, L.C.

Publication Date
1989-02-01

LBL-26717
Preprint

Center for Advanced Materials

CAM

Submitted to Journal of the American Ceramic Society

Sintering of Spherical Glass Powder under a Uniaxial Stress

M.N. Rahaman and L.C. De Jonghe

February 1989

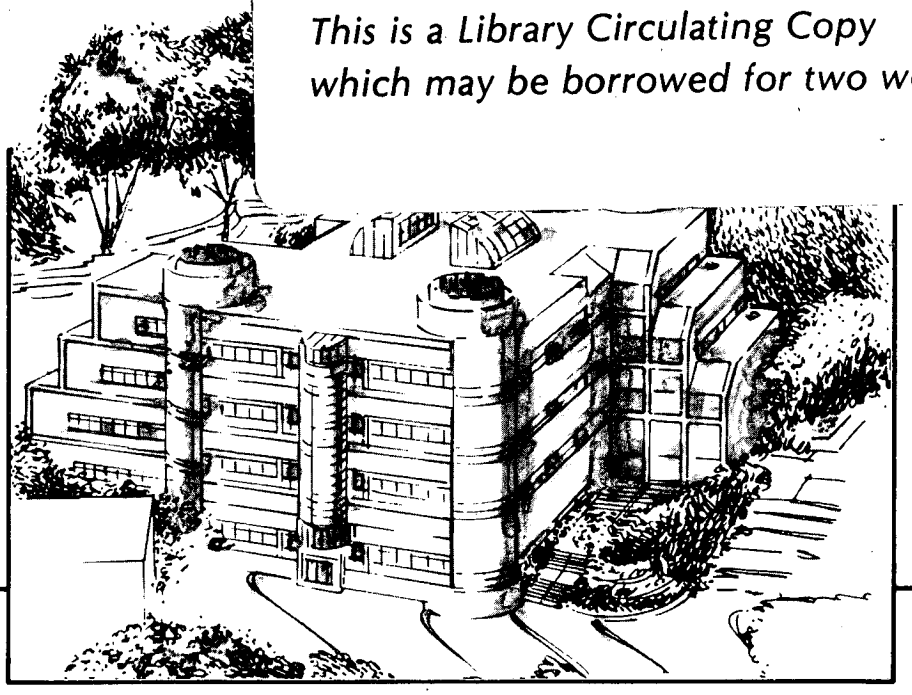

Materials and Chemical Sciences Division

Lawrence Berkeley Laboratory • University of California

ONE CYCLOTRON ROAD, BERKELEY, CA 94720 • (415) 486-4755

Prepared for the U.S. Department of Energy under Contract DE-AC03-76SF00098

DISCLAIMER

LBL # 26717

SINTERING OF SPHERICAL GLASS POWDER UNDER A UNIAXIAL STRESS

MOHAMED N. RAHAMAN*

Ceramic Engineering Department, University of Missouri-Rolla

Rolla, Missouri 65401

LUTGARD C. DE JONGHE*

Department of Materials Science and Mineral Engineering

University of California

and Center for Advanced Materials

Materials and Chemical Sciences Division

Lawrence Berkeley Laboratory

1 Cyclotron Road

Berkeley, CA 94720

This work was supported by the Division of Materials Science, Office of Basic Energy Sciences, U.S. Department of Energy, under Contract No. DE-AC03-76SF00098.

*Member, the American Ceramic Society.

Abstract

The sintering of spherical borosilicate glass powder (particle size 5-10 micron) under a uniaxial stress was studied at 800°C. The experiments allowed the measurement of the kinetics of densification and creep, the viscosities for creep and bulk deformation, and the sintering stress which was found to increase with density. The data show excellent agreement with Scherer's theory of viscous sintering. They are compared with earlier observations for a crushed soda-lime glass powder.

I. Introduction

The application of a controlled uniaxial stress to a powder compact during sintering was shown by Rahaman and De Jonghe[1-3] to be a powerful technique for the simultaneous measurement of densification and creep parameters and for providing an improved understanding of the sintering process. Later, Scherer[4] developed a formal theoretical analysis of the technique for the case of viscous sintering, and Venkatachari and Raj[5] utilized the same technique with relatively high stresses (i.e. sinter forging).

Earlier work by Rahaman et al[6] on crushed soda-lime glass powder provided the first experimental investigation of the effect of small, controlled uniaxial stress on the sintering of glass. Many of the observations (e.g. the ratio of the densification rate to the creep rate) were consistent with Scherer's model[7,8] for viscous sintering. A striking exception was the dependence of the creep viscosity on sintered density; the dependence was not only much stronger than is predicted by Scherer's theory but it was also much stronger than that found experimentally for polycrystalline materials.[3,5] Factors that might have led to the strong dependence included the highly lenticular nature of the porosity, a broad pore size distribution, alignment of the jagged, plate-like particles, or non-uniform removal of the binder.

Another surprising feature of the data was the direction of the anisotropic shrinkage; the samples shrank more in the axial direction which was the direction of pressing during formation of the sample. This is contrary to the observations of Giess et al[9,10] who found that jagged or spheroidized cordierite-type glass powders exhibited about the same 0.7 anisotropy of the ratio of the axial to the radial shrinkage for samples formed by pressing in

the axial direction. Thus anisotropic shrinkage is not a simple particle shape effect. It is highly likely that the factors that caused the anisotropy in the work of Rahaman et al also lead to the greater compliance in the axial direction.

The primary objective of the present work was to determine whether the strong dependence of the creep viscosity on density for the crushed glass powder was a general result and if so, to explore how it depends on anisotropic densification, pore morphology, and pore size distribution. To facilitate the interpretation of the data, the experiments utilized a well characterized, spherical glass powder with a relatively narrow particle size range (5-10 μm). A secondary objective was to extend the earlier work of Rahaman et al[6] to allow measurement of the bulk viscosity and the sintering stress of the porous glass compact and to explore their dependence on density. These parameters are important for checking available theories and for improving the understanding of sintering phenomena. For a brief review of past work on the sintering of glass, the reader is referred to the earlier paper by Rahaman et al.[6]

II. Experimental Procedure

The glass powder and experimental conditions used in the present work are different from those of the earlier work of Rahaman et al;[6] the procedure therefore needs to be described carefully. The commercially available borosilicate glass powder[#] used in the present work was spherical in shape and

---

[#]Corning 7070, MOSCI Corporation, Rolla, MO.

its diameter as measured using a particle size analyzer[+] was 8.0 ± 2.5 μm. Carbowax[*] (4 vol%) was used as a binder in the compaction of the powder. The amount of carbowax was approximately the minimum required to produce samples that were strong enough to be handled and was about half of that used previously.[6] The carbowax was dissolved in chloroform, then the required amount of glass powder was added, and the mixture was stir-dried. The dried powder was disrupted in an agate mortar and pestle and then pressed at ≈ 25 MPa into cylindrical compacts (6 mm in diameter by 5 mm) with the same density of 0.61 ± 0.01 of the theoretical.

Binder removal from all the samples was performed at the same time and under identical conditions. The samples were placed on a platinum sheet (with the axial pressing direction along the vertical) and the temperature was raised by 50°C every 10 min up to 400°C. After 30 min at this temperature, the samples were lightly presintered by heating up to 700°C for 5 min; the presintering step was necessary in order to make the samples strong enough for subsequent manipulation. The shrinkage at the end of the presintering step was < 1% and the density of the samples was 0.63 ± 0.01.

Sintering was performed in an inert atmosphere (argon gas flowing at 50 cm^3/min) and the sample was separated from the dilatometer pushrods by high purity graphite foil. Platinum foil could not be used because of extensive reaction with the glass which leads to sticking and to a dumbell-shaped sintered sample in which the regions near the contact surfaces shrank less

---

[*]Union Carbide Corp., New York, NY.

[+]Model CAPA-700, Horiba Instruments Inc., Irvine, CA.

than the other regions. Sintering was performed in a loading dilatometer;[1] the sample was placed between the pushrods and inserted quickly into the hot zone of the furnace that was kept at a fixed temperature to produce an "isothermal" sample temperature of 800°C. This temperature was chosen in order to achieve a sintered density of > 0.95 after ≈ 2 hours. The axial direction of the sample was along the horizontal.

Samples were sintered with or without a controlled, externally applied uniaxial stress. For sintering under an external stress, the load was applied to the sample rapidly (< 5 s) at the commencement of shrinkage and the axial shrinkage and temperature were monitored continously. The load on the sample was 0.75 N and, with the spring load of the dilatometer pushrod, this resulted in an initial stress of 34 kPa. In a separate set of experiments, sintering was terminated after times between 0 and 2 hours and the axial and radial dimensions of these samples were measured using a micrometer.

Sintering without an external stress was performed intermittently in order to remove the effects of the dilatometer spring load. The samples were sintered under a temperature schedule that was identical to that for the samples sintered under load; the main difference was that they were not in contact with the dilatometer pushrods. Ten samples were sintered for times between 0 and 2 hours and their mass and dimensions were measured before and after each run.

The final densities of the samples were verified using Archimedes' principle and the microstructures of representative samples were examined using scanning electron microscopy. As pointed out earlier, the spring load of the dilatometer pushrod imposed an additional load on the samples sintered under an external stress; this load is not negligible and also varies with the

shrinkage of the sample. The procedure used to measure the spring load was identical to that outlined earlier.[6]

III. Data Analysis

The analysis of the present data was almost identical to that outlined earlier;[6] only the main relations will be summarized here.

The experiments give data for the axial and radial shrinkages from which the true strains in the axial and radial directions, ϵ_z and ϵ_r, respectively, were calculated according to the relations

$$\dot{\epsilon}_z = d[\ln (L/L_o)]/dt \tag{1}$$

$$\dot{\epsilon}_r = d[\ln (R/R_o)]/dt \tag{2}$$

where L_o and R_o are the initial length and radius, respectively, and L and R are the corresponding time-dependent values.

The creep strain rate, $\dot{\epsilon}_c$, and the volumetric strain rate, $\dot{\epsilon}_\rho$, were evaluated according to the relations[11]

$$\dot{\epsilon}_c = (2/3)(\dot{\epsilon}_z - \dot{\epsilon}_r) \tag{3}$$

$$\dot{\epsilon}_\rho = \dot{\rho}/\rho = -(\dot{\epsilon}_z + 2\dot{\epsilon}_r) \tag{4}$$

where ρ is the relative density.

The axial stress, σ_z, on the sample was measured from the constant applied load, P, the variable spring load, S, and the change in cross-sectional area of the sample.[6] If the sintering (or densification) stress due to reduction in surface area is defined as Σ, then the mean hydrostatic stress, σ_h, experienced by the sample under uniaxial load of σ_z is

$$\sigma_h = \Sigma + \sigma_z/3 \tag{5}$$

In earlier publications, the sintering stress was denoted Σ/ϕ, where ϕ is

referred to as the stress intensification factor.[12-14] With the present notation Σ is equivalent to Σ/ϕ used in earlier work. The change adopted here then uses the same notation as found in related work.[7,8]

IV. Results

Figure 1 shows the results for ϵ_z vs time, t, for the samples sintered at 800°C under an initial uniaxial stress, σ_{zo}, of 34 kPa and under zero external stress. As pointed out earlier, ϵ_z for the sample sintered under stress was measured continuously; the data shown are the average of two runs under identical conditions and at any time, the strain values are reproducible to within ± 0.01. The load on the sample was applied at t = 0 and the sintering temperature was reached after t = 5 min. Ten samples were sintered under zero load for the different times shown.

Figure 2 shows the results for ϵ_z vs ϵ_r for the samples sintered with and without a uniaxial stress. For the sample sintered under stress, ϵ_r is very small. The use of significantly higher stresses produced barrel-shaped samples from which accurate data for ϵ_r could not be obtained. The data for the sample sintered without stress fall below the projected curve for isotropic shrinkage i.e. the sample shrinks more in the radial direction; the ratio ϵ_z/ϵ_r varies from 0.6 initially to 0.7 after 2 hours of sintering.

Smooth curves were fitted through the data of Figs. 1 and 2 and ϵ_c and ρ were evaluated according to Eqs. (3) and (4). The results for ϵ_c and ρ are shown in Figs. 3 and 4, respectively. The data for ϵ_c for the sample sintered without load reflect the anisotropic nature of the shrinkage. Figure 4 shows that a measureable increase in the sample density was produced by the applied

stress. The final densities of the samples sintered with and without stress are 0.99 and 0.97, respectively; these values are within 2% of those found using Archimedes' principle. The theoretical density of Corning 7070 borosilicate glass used in this study is given[15] as 2.13 g/cm^3.

Data for $\dot{\epsilon}_c$ and $\dot{\epsilon}_\rho$ were obtained by fitting smooth curves to the data of Figs. 1 and 2 followed by differentiating according to Eqs. (3) and (4). The results are shown in Fig. 5 as a function of ρ for the samples sintered under an initial stress of 34 kPa and under zero stress. As pointed out earlier, the stress on the sample changes due to decreases in the dilatometer spring load and the cross-sectional area. At this stage, the data of Fig. 5 have not been normalized to account for the varying uniaxial stress. The uniaxial stress on the sample, σ_z, as a function of ϵ_z is shown in Fig. 6. (The data of Figs. 1 and 4 can be used to evaluate σ_z vs ρ.) It is seen that σ_z decreases from 34 to 21 kPa during the experiment.

Figure 7(a) shows a scanning electron micrograph of a fracture surface of a powder compact pressed with binder to a density of 0.61. The particles are seen to be spherical and most have diameters between 5 and 10 μm. It should be noted that no particle fractures have resulted from the powder compaction process. A scanning electron micrograph of a polished surface of a sample sintered without load to a density of $\approx$ 0.85 is shown in Fig. 7(b). The pore shape is somewhat less lenticular than that observed earlier[6] for the sintering of crushed glass.

V. Discussion

The present data on spherical borosilicate glass powder (Fig. 2) show the

expected shrinkage anisotropy, i.e. the sample shrinks less in the axial direction which is the direction of pressing during formation of the green compact. This is quite different from the results of earlier work by Rahaman et al[6] on crushed glass powder in which the sample shrank more in the axial direction. As pointed out earlier, the unexpected shrinkage anisotropy observed by Rahaman et al might be due to a number of effects, including particle shape, particle size distribution, particle alignment, and non-uniform binder burnout. The work of Geiss et al[9,10] and the analysis of their data by Exner and Geiss[16] show that anisotropic shrinkage is not a simple particle shape effect, a particle size effect or a temperature effect. Although the particle size distribution of the classified, crushed glass used in the earlier work was not measured, scanning electron micrographs of the powder indicate that it is comparable to that of the spherical glass powder of the present work. Thus it appears highly likely that particle alignment produced during compaction of the angular particles was the cause of the unexpected shrinkage anisotropy observed by Rahaman et al. Indeed, micrographs of the powder (Ref. 6, Fig. 10) show a significant fraction of elongated particles. Although care was taken to remove the binder slowly, it is possible that the higher binder content used in the earlier work (8 v% compared to 4 v%) could have also contributed to the unexpected shrinkage anisotropy through enhancement of particle alignment.

The strain anisotropy ratio, ϵ_z/ϵ_r, of Fig. 2 varies from 0.6 initially to 0.7 at the end of the experiment. This is comparable to the shrinkage anisotropy observed by Giess[9,10] for cordierite-type glass powder in the intermediate and final stages of sintering. The lower shrinkage anisotropy observed by Giess in the earlier stages of sintering is most likely due[17] to

the much larger compaction pressures used (75-150 MPa compared to 25 MPa in the present work).

As outlined earlier, a primary objective of the present work was to investigate whether the drastic dependence of the creep viscosity and the densification rate, observed in the earlier work on crushed soda-lime glass powder, was a general result. The analysis of the results will follow the treatment provided earlier by Rahaman et al[6] and only the important relations required for the present discussion will be outlined.

According to Scherer[7] the "free" densification rate, $\dot{\epsilon}_{\rho f}$, (i.e. under zero applied stress) is given by

$$\dot{\epsilon}_{\rho f} = (k/\eta)[(3\pi)^{1/3}/2](2 - 3cx)/[x^{1/3}(1 - cx)^{2/3}] \qquad (6)$$

where η is the viscosity of the bulk glass, c is a numerical constant equal to $8\sqrt{2}/(3\pi)$, x is equal to a/l where a is the radius and l the length of the cylinders of the model (consisting of cylinders in a cubic array), and k is a material constant equal to $\gamma/(l_o\rho_o^{1/3})$ where γ is the surface tension of the glass, and l_o and ρ_o are the initial length and density, respectively, of the model unit cell. In fig. 8 the results for $\dot{\epsilon}_{\rho f}$ vs ρ are compared with the predictions of Eq. (6). The material constants k and η have been chosen arbitrarily to give equality between theory and experiment at $\rho = 0.8$; this leads to a value of -44.3×10^{-4} min^{-1} for the ratio k/η. It is seen that the present data are very consistent with Scherer's theory.

Scherer's analysis[8] shows that $\dot{\epsilon}_c$ and $\dot{\epsilon}_\rho$ can be written as

$$\dot{\epsilon}_c = (2/3)[(\dot{\epsilon}_{fz} - \dot{\epsilon}_{fr}) + (1 + N)\sigma_z/F] \qquad (7)$$

$$\dot{\epsilon}_\rho = -(\dot{\epsilon}_{fz} + 2\dot{\epsilon}_{fr}) - (1 - 2N)\sigma_z/F \qquad (8)$$

where $\dot{\epsilon}_{fz}$ and $\dot{\epsilon}_{fr}$ are the "free" strain rates in the axial and radial directions (i.e. for a sample sintered under zero applied stress), σ_z is the

applied uniaxial stress, and F and N are the resistance to flow (or "effective modulus") and "effective Poisson's ratio", respectively, given by

$$F \approx 3\eta\rho/(3 - 2\rho) \tag{9}$$

$$N \approx 0.5[\rho/(3 - 2\rho)]^{1/2} \tag{10}$$

The present results will be discussed in terms of a "creep viscosity", η_c, and a "bulk viscosity", η_ρ, of the porous powder compact (i.e. the viscous response of the compact to a hydrostatic stress) that are related to F and N according to the relations

$$\eta_c = 3F/[2(1 + N)] \tag{11}$$

$$\eta_\rho = F/[3(1 - 2N)] \tag{12}$$

Experimental results for η_c and η_ρ were evaluated from the data of Figs. 1, 2 and 6 according to Eqs. (7) and (8) and compared with the theoretical predictions given by Eqs. (9) - (12); these data and those for η_ρ/η_c are shown as a function of ρ in Fig. 9. It is seen that the data provide excellent confirmatiom of the predictions of Scherer's theory. If the data for η_c are extrapolated to $\rho = 1$, then the viscosity of the bulk glass, η, is found to be 4.7 MPa min (2.8×10^9 poise); with the value found earlier for k/η, this gives k = -21.4 kilopascal.

The consistency of η_ρ and η_c with Scherer's predictions found in the present work is quite different from the earlier work of Rahaman et al[6] on crushed glass. This, together with the the expected shrinkage anisotropy observed in the present work, supports the original suggestion that the factors that caused the unexpected shrinkage anisotropy in the earlier work also lead to the greater compliance in the axial direction. As pointed out earlier, the main factor that caused the unexpected shrinkage anisotropy in the earlier work appears to be particle alignment; it is also possible that

the higher binder content could have contributed to the enhancement of the effect. Although it was not investigated in the earlier work, loss of soda from the crushed soda-lime glass powder during sintering could have also produced changes in the viscosity.

The ratio η_ρ/η_c increases by a factor of ≈ 3 in the intermediate stage of sintering ($\rho \approx 0.65$-0.9) and then increases rapidly at higher density; if the same relationship holds for polycrystalline materials, then the assumption of Rahaman et al[3] that $\eta_\rho/\eta_c \approx 1$ provides a good estimate of the sintering stress within the intermediate stage of sintering.

The present data allow the measurement of the sintering stress, Σ, due to reduction of surface area; Σ is defined by

$$\Sigma = -\eta_\rho(\dot{\epsilon}_{fz} + 2\dot{\epsilon}_{fr}) \qquad (13)$$

The data of Figs. 1 and 9 were used to evaluate Σ. According to Scherer's theory[8] the sintering stress is given by

$$\Sigma = -k[3\pi^4 x^5/(1 - cx)^2]^{1/3} \qquad (14)$$

where the symbols k,x, and c have been defined by Eq. (6); k has been found earlier and is equal to -21.4 kilopascal for the present work. The experimental and theoretical values for Σ as a function of ρ are compared in Fig. 10; it is seen that the data are consistent with Scherer's theory.

The ratio of the densification rate to the creep rate, found to be nearly constant in the earlier work[6] (in agreement with Scherer's theory) can also be measured. The creep strain rate, $\dot{\epsilon}_{c\sigma}$, due to a uniaxial stress, σ_z, was evaluated from the data of Figs. 6 and 9 according to the relation

$$\dot{\epsilon}_{c\sigma} = \sigma_z/\eta_c \qquad (15)$$

The data for $\dot{\epsilon}_{c\sigma}$ were evaluated at a constant initial stress of 34 kPa. The "free" densification rate, $\dot{\epsilon}_{\rho f}$, was measured earlier (Fig. 6). The theoretical

values for $\dot{\epsilon}_{\rho f}$ and $\dot{\epsilon}_{c\sigma}$ were taken from Eqs. (6) and (11). Figure 11 shows a comparison of the experimental and theoretical results for the ratio $\dot{\epsilon}_{\rho f}/\dot{\epsilon}_{c\sigma}$ as a function of ρ; the data are in good agreement with Scherer's theory. The relatively constant value for this ratio within the intermediate stage of sintering has also been found in systems where the mechanism of mass transport is solid state diffusion or diffusion through a liquid phase.[18]

The results of the present work on spherical, borosilicate glass powder provide excellent confirmation of Scherer's theory of viscous sintering. Further work is in progress on crushed glass powder of the same composition in order to determine the cause of the significant deviations from theory and the unexpected shrinkage anisotropy observed in earlier work. The present work indicates that particle alignment and its possible enhancement by binder content should be investigated.

VI. Conclusions

The present work, in which a spherical borosilicate (Corning 7070) glass powder was sintered under a uniaxial stress, allowed the measurement of the kinetics of densification and creep, the creep and bulk viscosities, and the sintering stress. The data are consistent with the predictions of Scherer's theory of viscous sintering and also show the expected shrinkage anisotropy i.e. the sample shrinks less in the axial direction which is the direction of pressing during the formation of the green samples.

Particle alignment appears to be the main cause of the unexpected shrinkage anisotropy (i.e. the samples shrank more in the axial direction) and the greater compliance of the samples (i.e. to the drastic deviation of the

measured creep viscosity from the predictions of Scherer's theory) that were observed in the earlier work of Rahaman et al[6] on crushed, soda-lime glass powder. The higher binder content used in the earlier work could have contributed to the enhancement of particle alignment.

Acknowledgement: The experimental phase of this work was performed in the Lawrence Berkeley Laboratory when Dr. M. N. Rahaman was a visiting staff scientist in the Materials and Chemical Sciences Division.

References

1. L. C. De Jonghe and M. N. Rahaman, "A Loading Dilatometer," Rev. Sci. Instrum., 55 [12] 2007-10 (1984)

2. M. N. Rahaman and L. C. De Jonghe, "Sintering of CdO Under Low Applied Stress," J. Am. Ceram. Soc., 67 [10] C-205--C207 (1984).

3. M. N. Rahaman, L. C. De Jonghe, and R. J. Brook, "Effect of Shear Stress on Sintering," J. Am. Ceram. Soc., 69 [1] 53-58 (1986).

4. G. W. Scherer, "Viscous Sintering Under a Uniaxial Load," J. Am. Ceram. Soc., 69 [9] C-206--C-207 (1986).

5. K. R. Venkatachari and R. Raj, "Shear Deformation and Densification of Powder Compacts," J. Am. Ceram. Soc., 69 (6) 499-506 (1986).

6. M. N. Rahaman, L.C. De Jonghe, G. W. Scherer, and R. J. Brook, "Creep and Densification During Sintering of Glass Powder Compacts," J. Am. Ceram. Soc., 70 [10] 766-74 (1987).

7. G. W. Scherer, "Sintering of Low-Density Glasses: I, Theory," J. Am. Ceram. Soc., 60 [5-6] 239-43 (1977).

8. G. W. Scherer, "Sintering of Inhomogeneous Glasses: Application to Optical Waveguides," J. Non-Cryst. Solids, 34 239-56 (1979).

9. E. A. Giess, J. P. Fletcher, and L. W. Herron, "Isothermal Sintering of Cordierite-Type Glass Powders," J. Am. Ceram. Soc., 67 [8] 549-52 (1984).

10. E. A. Giess, C. F. Guerci, G. F. Walker, and S. H. Wen, "Isothermal Sintering of Spheroidized Cordierite-Type Glass Powders," J. Am. CEram. Soc., 68 [12] C-328--C-329 (1985).

11. R. Raj, "Separation of Cavitation Strain and Creep Strain During Deformation," J. Am. Ceram. Soc., 65 [3] C-46 (1982).

12. W. Beere, "A Unifying Theory of the Stability of Penetrating Liquid Phases and Sintering Pores," Acta Metall., 23 [1] 131-38 (1975).

13. W. Beere, "The Second Stage Sintering Kinetics of Powder Compacts," Acta Metall., 23 [1] 139-45(1975).

14. J. M. Vieira and R. J. Brook, "Kinetics of Hot-Pressing: The Semilogarithmic Law," J. Am. Ceram. Soc., 67 [4] 245-49 (1984).

15. Handbook of Glass Properties, edited by N. P. Bansal and R. H. Doremus. Academic, Orlando, 1986.

16. H. E. Exner and E. A. Giess, "Anisotropic Shrinkage of Cordierite-Type Glass Powder Cylindrical Compacts," J. Mater. Res., 3 [1] 122-25 (1988).

17. H. E. Exner, "Principles of Single Phase Sintering," Rev. Powder Metall. Phys. Ceram., 1 [1-4] 1-251 (1979).

18. M-Y. Chu, L. C. De Jonghe, and M. N. Rahaman, "Effect of Temperature on the Densification/Creep Rate During Sintering," Acta Metall., to be published.

Figure Captions

Fig. 1. Axial strain vs time for a borosilicate glass powder (Corning 7070) sintered at 800°C under an initial uniaxial stress of 34 kPa and under zero stress. The data for the sample sintered under stress were measured continuously and the strain values were reproducible to within ± 0.01, as indicated for various times.

Fig. 2. Axial strain vs radial strain for the experiments described in Fig. 1.

Fig. 3. Creep strain vs time calculated from Figs. 1 and 2 and Eq. (3).

Fig. 4. Relative density vs time calculated from Figs. 1 and 2 and Eq. (4).

Fig. 5. Creep rate and densification rate vs relative density for samples sintered under an initial stress of 34 kPa and under zero stress.

Fig. 6. Applied uniaxial stress vs uniaxial strain.

Fig. 7. Scanning electron micrographs of (a) a fracture surface of the green sample, and (b) a polished surface of a sample sintered to a relative density of ≈ 0.85.

Fig. 8. Comparison of the experimental data for the "free" densification rate vs relative density with the predictions of Scherer's theory given in Eq. (6).

Fig. 9. Comparison of the experimental data for the creep viscosity, η_c, the bulk viscosity, η_ρ, and the ratio η_ρ/η_c vs relative density with the predictions of Scherer's theory given in Eqs. (9) - (12).

Fig. 10. Experimental data for the sintering stress vs relative density compared with the predictions of Scherer's theory given in Eq. (14).

Fig. 11. Ratio of the "free" densification rate to the creep rate (normalized to a constant uniaxial stress of 34 kPa) vs relative density compared with the predictions of Scherer's theory given in Eqs. (6), (11), and (15).

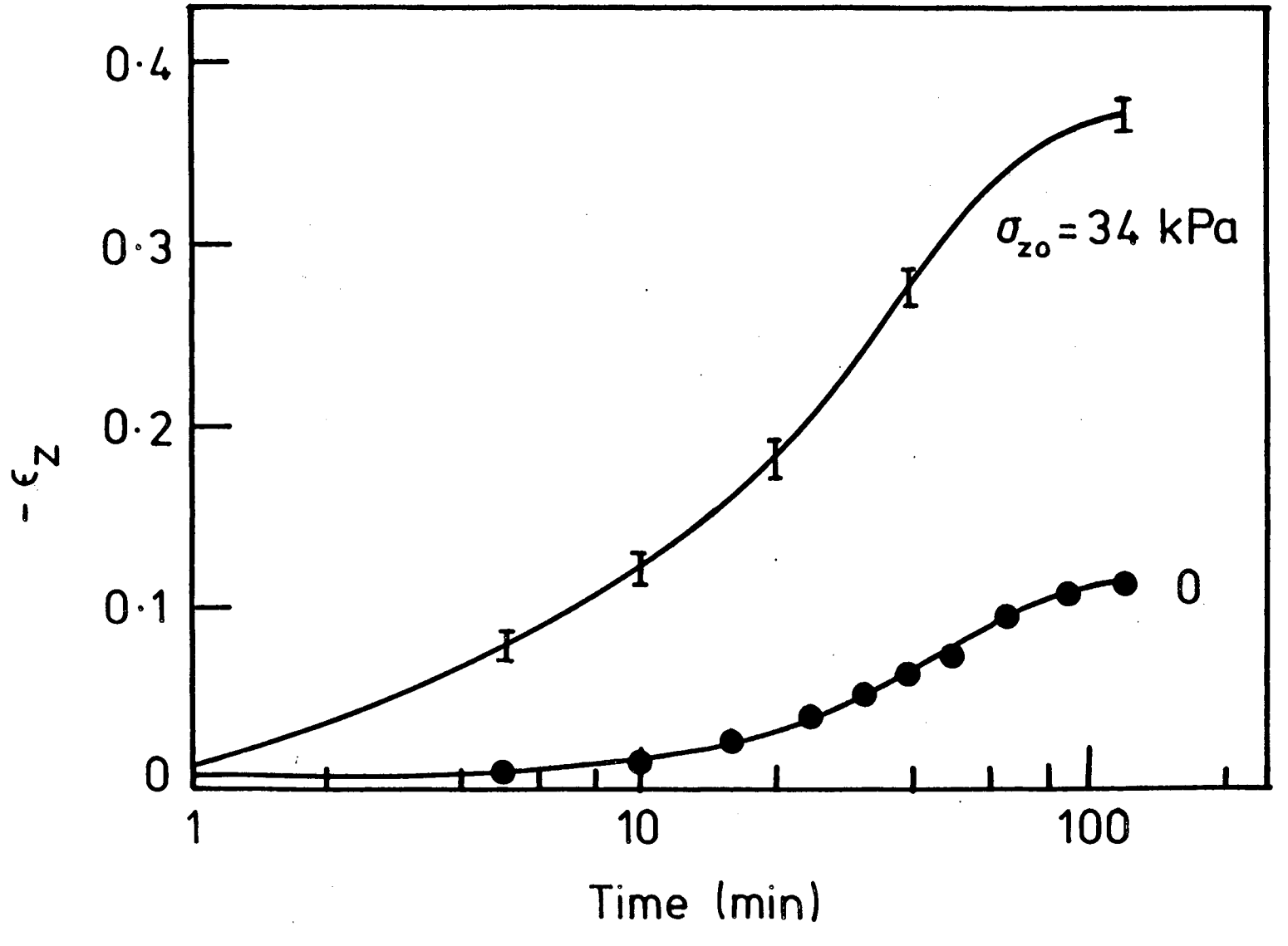

Figure 1

XBL 892-422

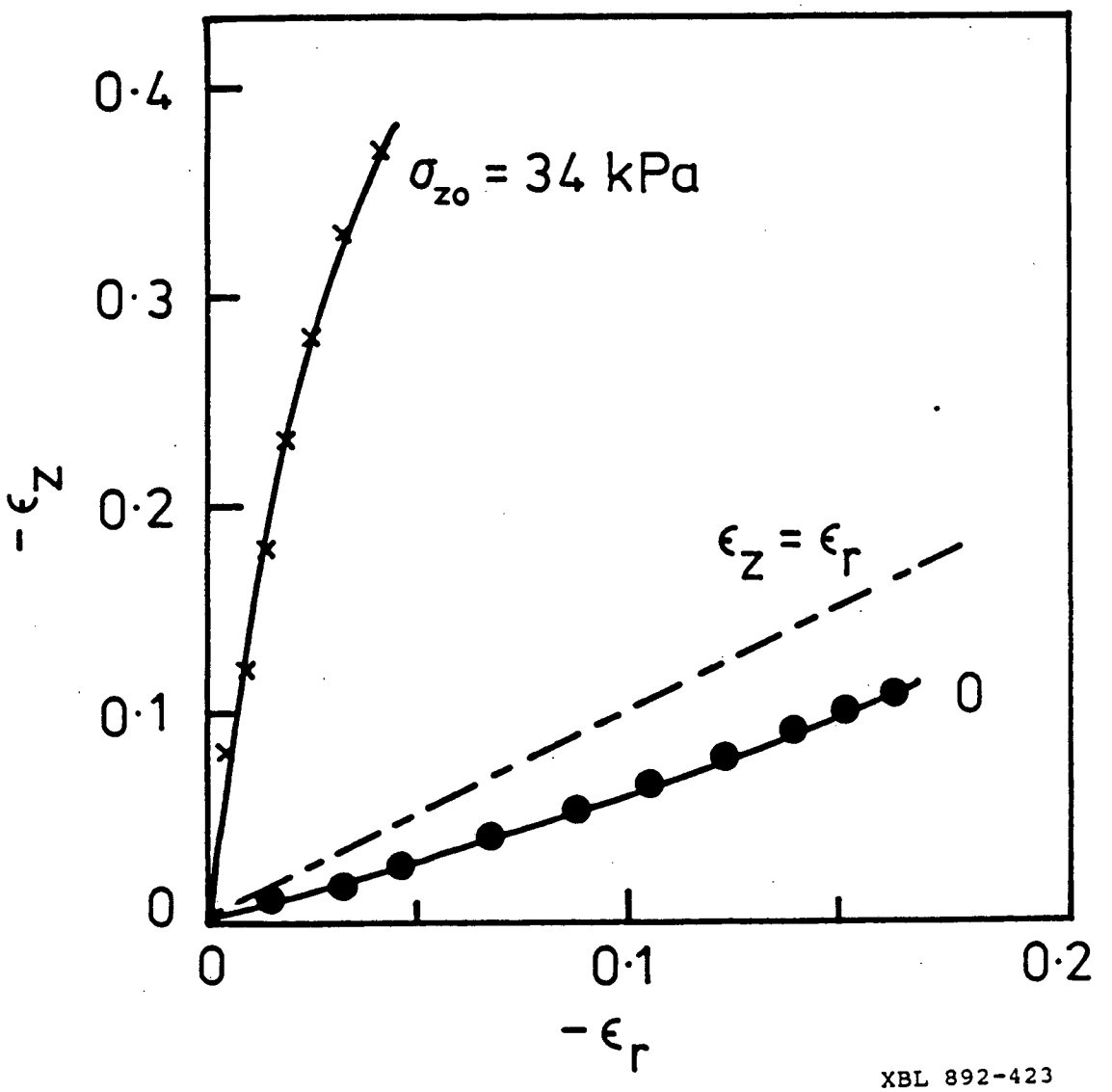
0·4
0·3
0·2
0·1
0
$-\epsilon_z$
σ_{zo} = 34 kPa
$\epsilon_z = \epsilon_r$
0
0
0·1
0·2
$-\epsilon_r$
XBL 892-423

Figure 2

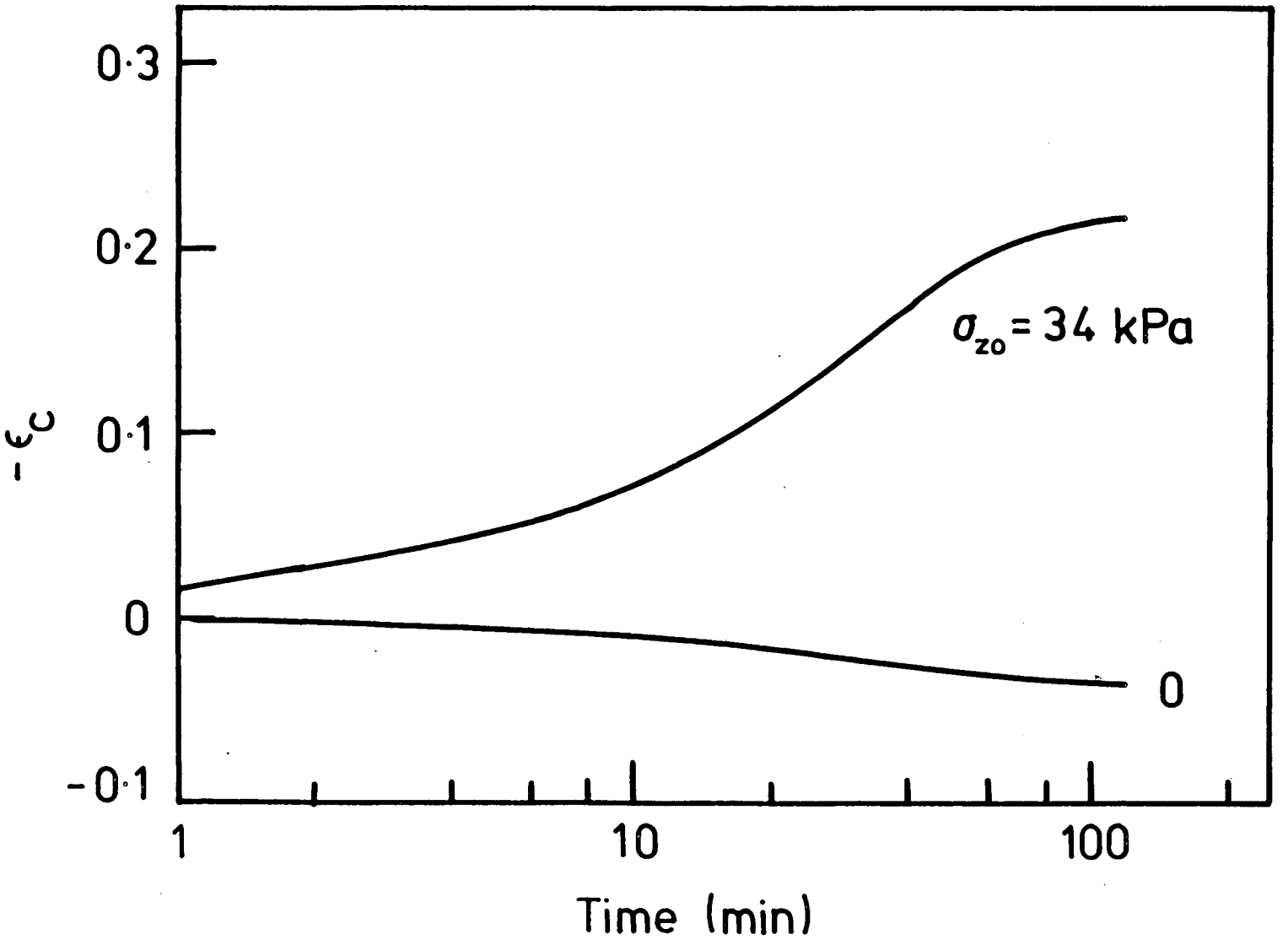

XBL 892-424

Figure 3

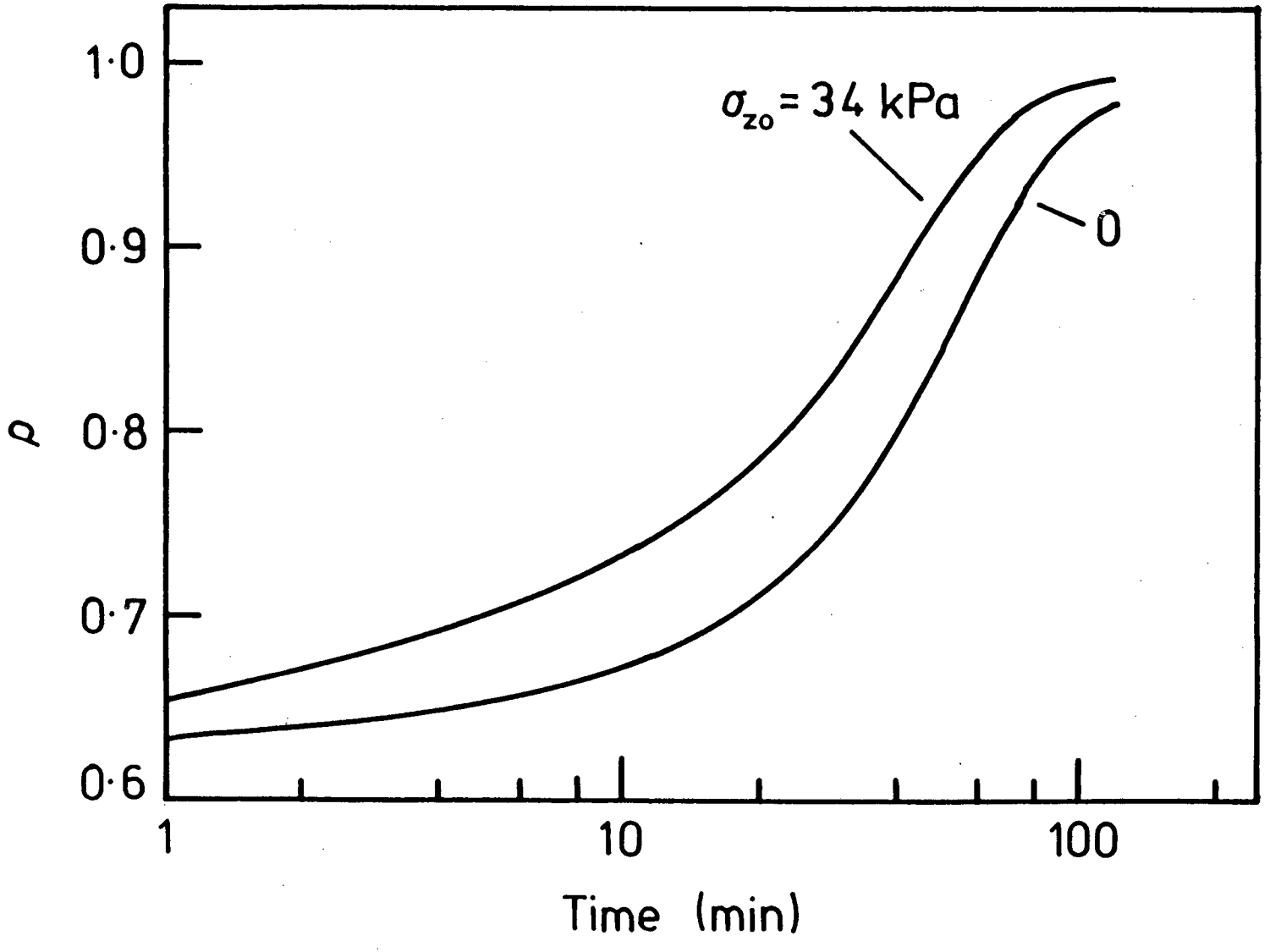

XBL 892-425

Figure 4

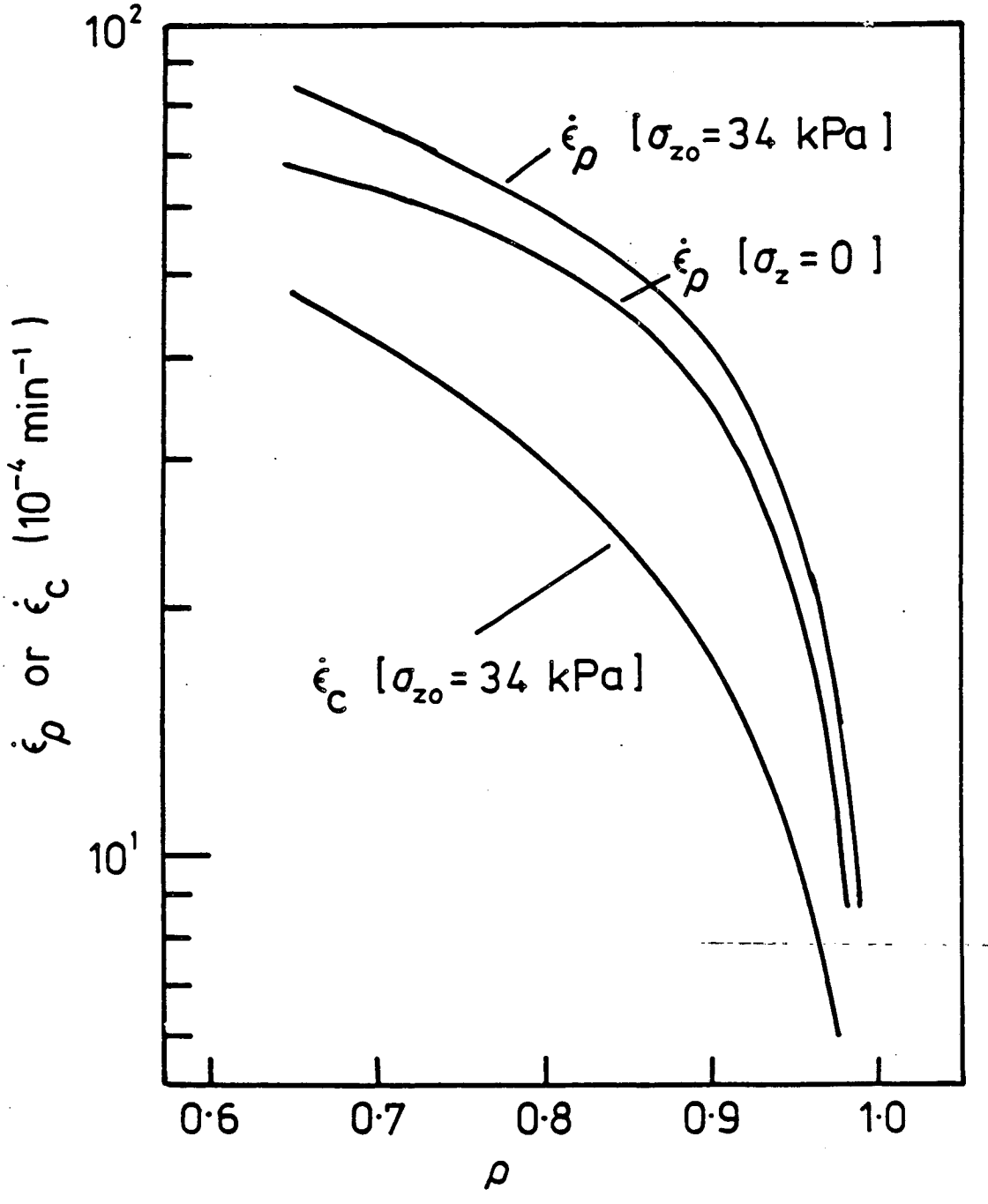

XBL 892-426

Figure 5

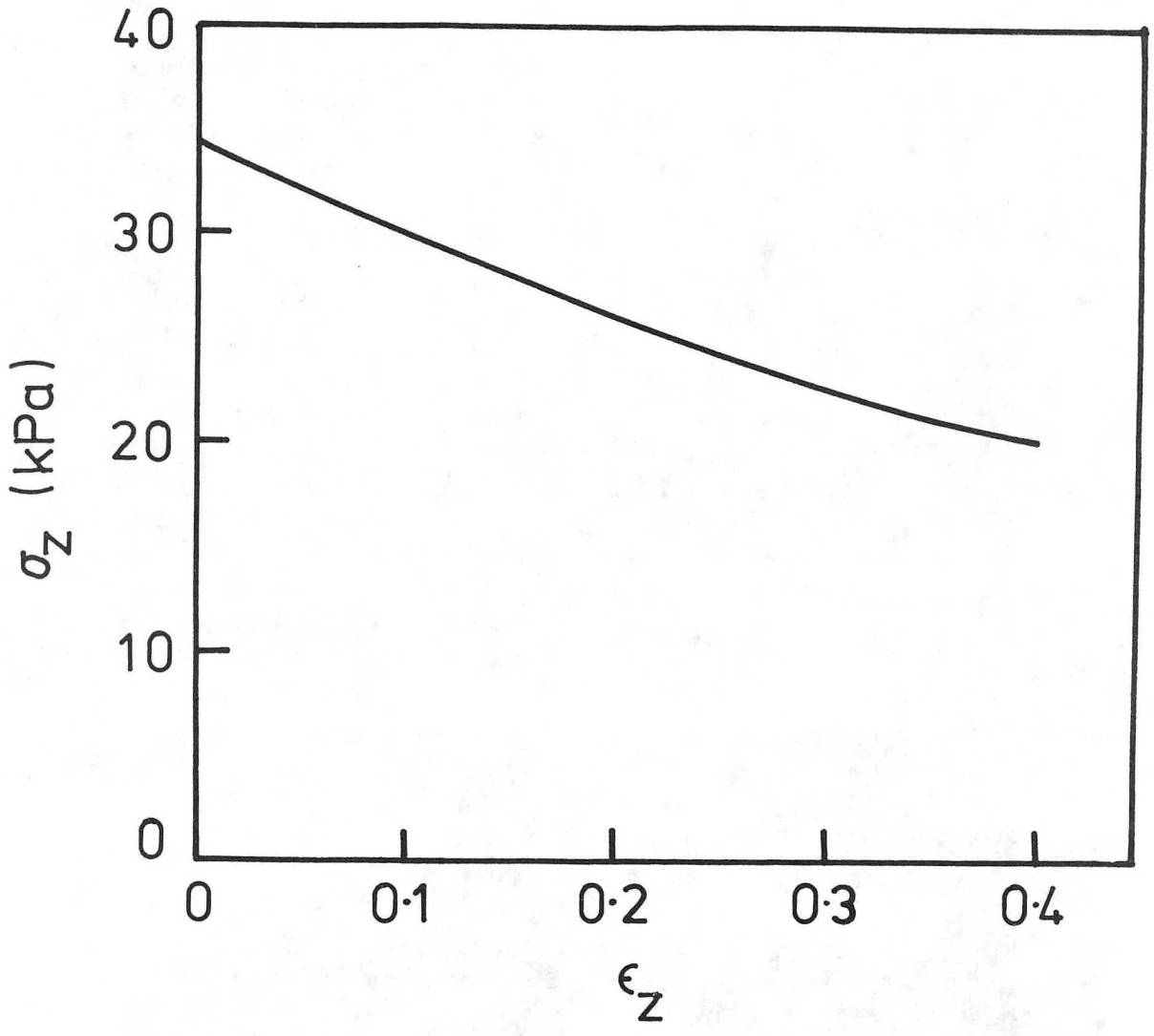

XBL 892-427

Figure 6

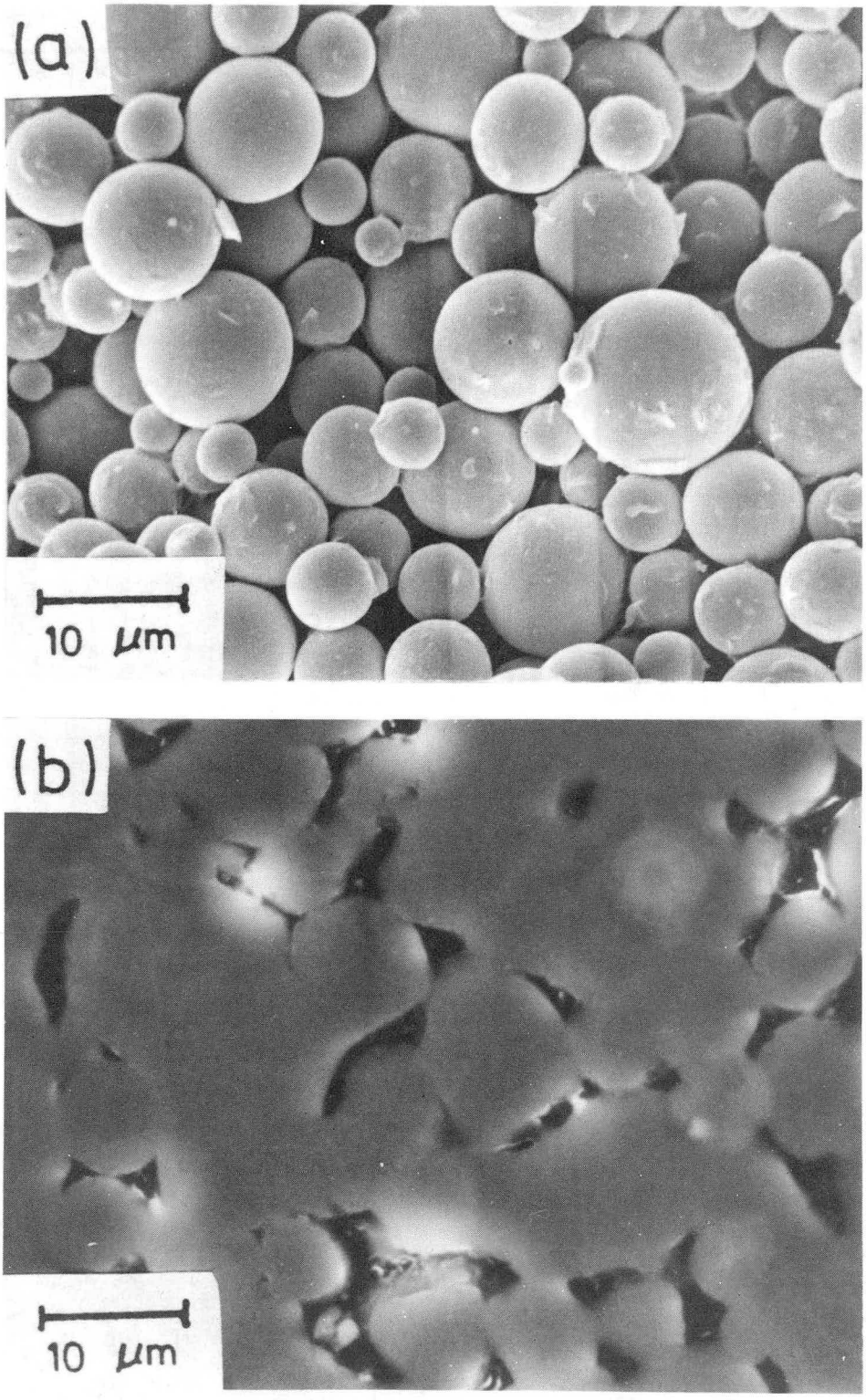

Figure 7

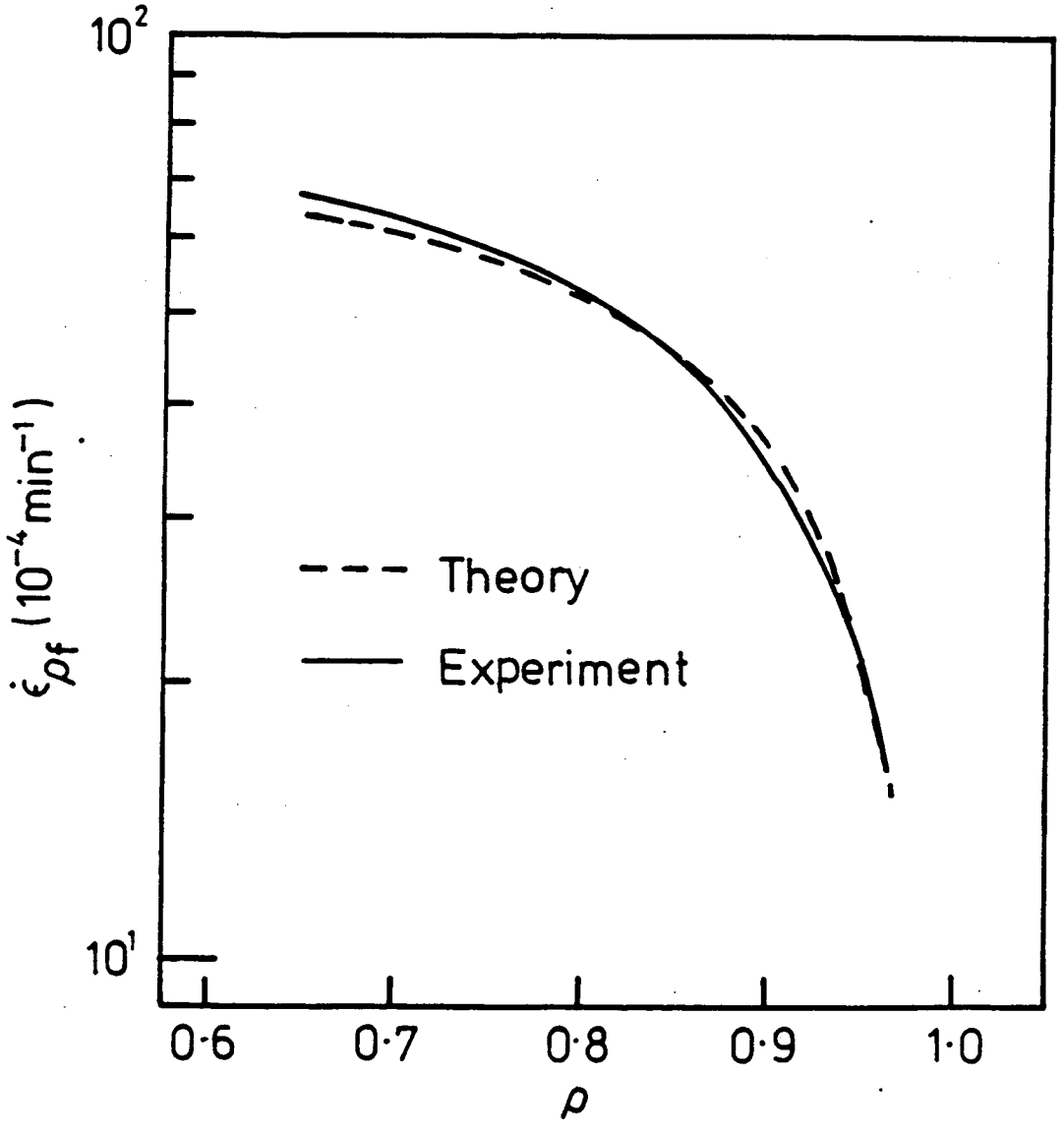

XBL 892-428

Figure 8

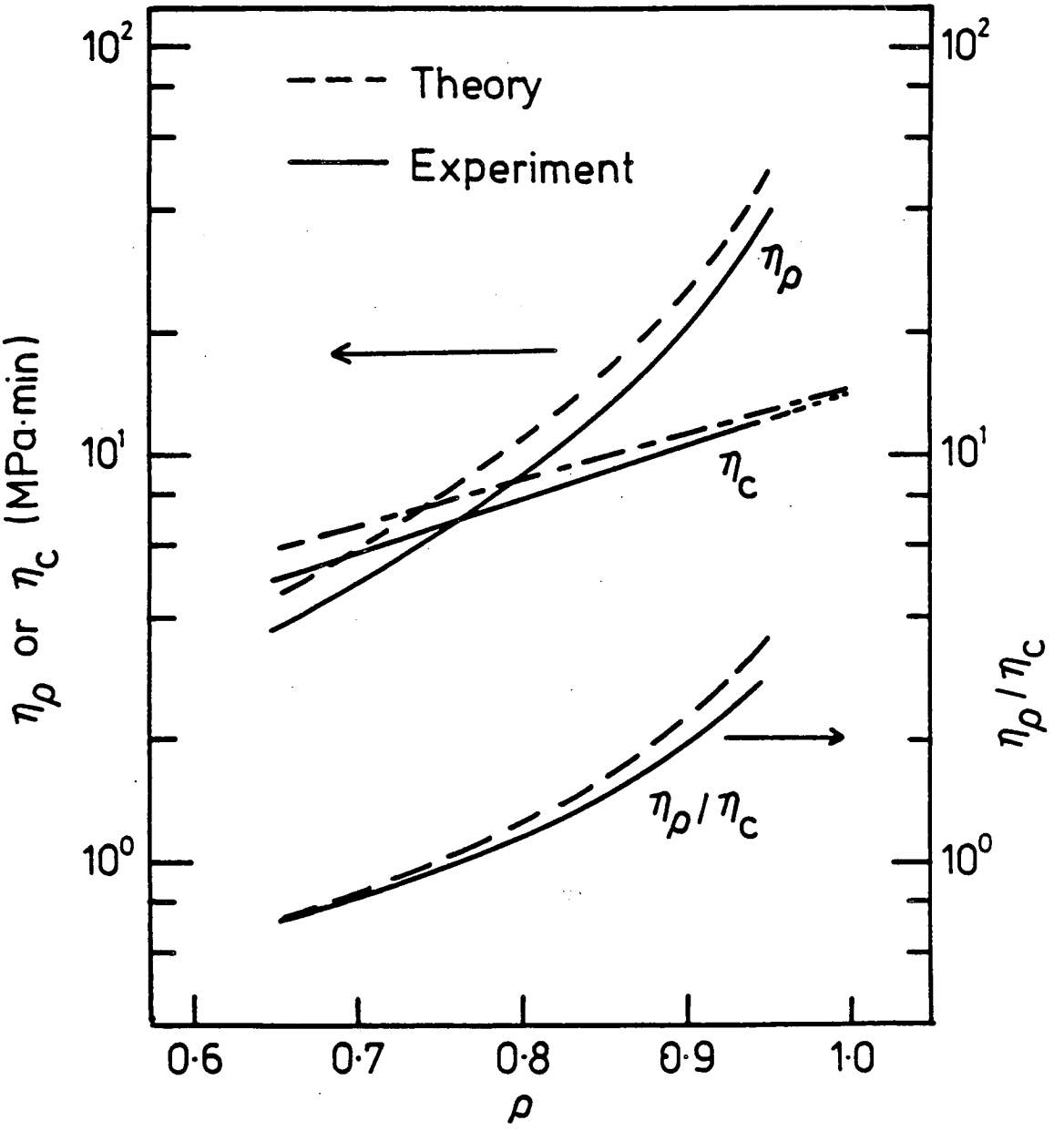
Theory
Experiment
η_ρ
η_c
η_ρ / η_c
η_ρ or η_c (MPa·min)
η_ρ / η_c
10^2
10^1
10^0
0·6
0·7
0·8
0·9
1·0
ρ
XBL 892-429

Figure 9

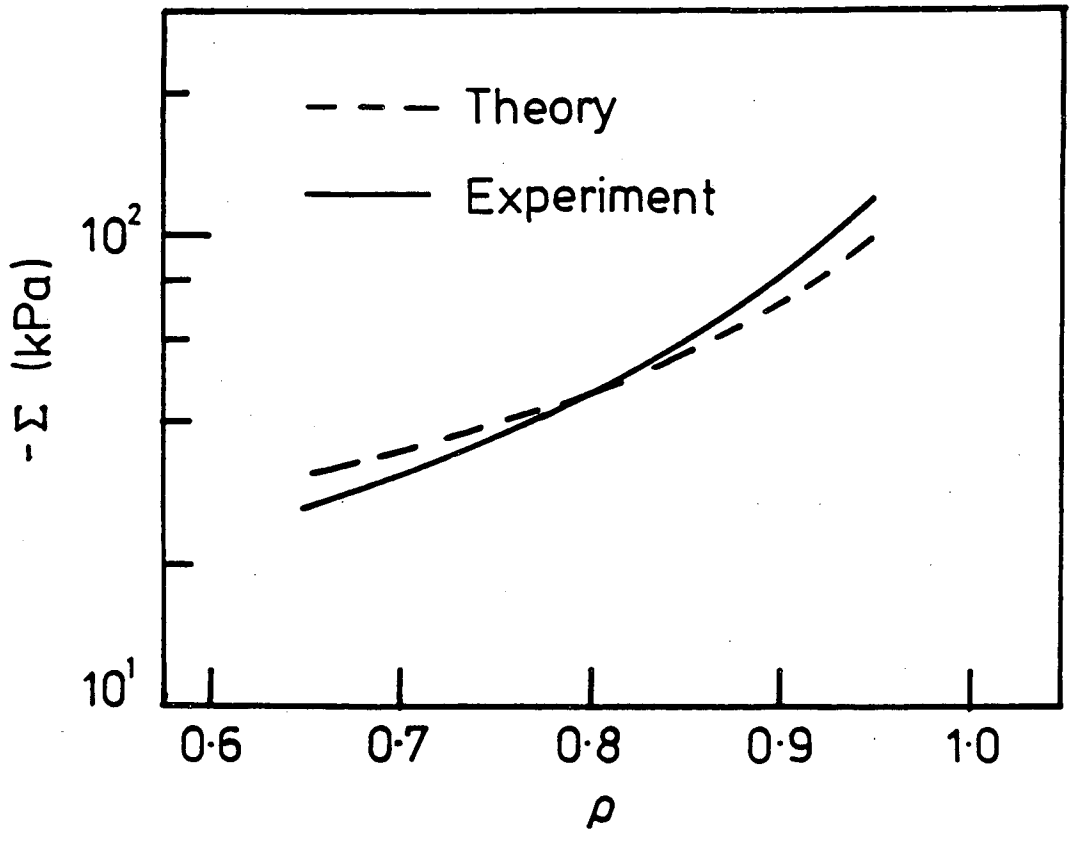

XBL 892-430

Figure 10

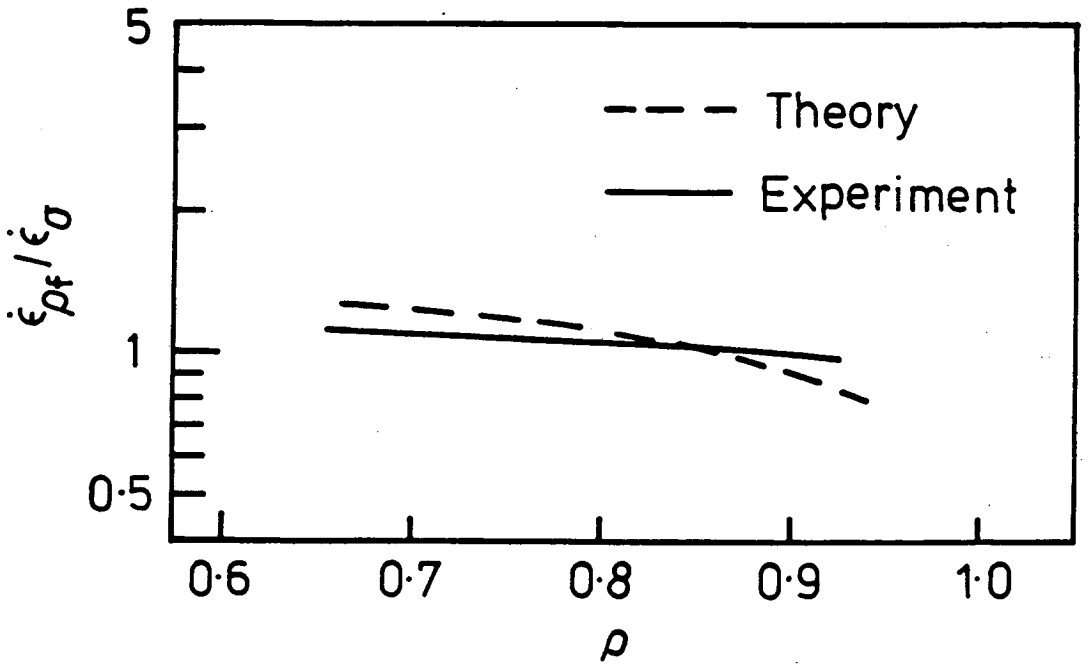

XBL 892-431

Figure 11

LAWRENCE BERKELEY LABORATORY
CENTER FOR ADVANCED MATERIALS
1 CYCLOTRON ROAD
BERKELEY, CALIFORNIA 94720